Dispersion rheology of carbon nanotubes in a polymer matrix

Y. Y. Huang, S. V. Ahir, and E. M. Terentjev
Cavendish Laboratory, University of Cambridge, J.J. Thomson Avenue, Cambridge CB3 OHE, United Kingdom
(Received 4 December 2005; revised manuscript received 30 January 2006; published 23 March 2006)

We report on rheological properties of a dispersion of multiwalled carbon nanotubes in a viscous polymer matrix. Particular attention is paid to the process of nanotubes mixing and dispersion, which we monitor by the rheological signature of the composite. The response of the composite as a function of the dispersion mixing time and conditions indicates that a critical mixing time t^* needs to be exceeded to achieve satisfactory dispersion of aggregates, this time being a function of nanotube concentration and the mixing shear stress. At shorter times of shear mixing $t<t^*$, we find a number of nonequilibrium features characteristic of colloidal glass and jamming of clusters. A thoroughly dispersed nanocomposite, at $t>t^*$, has several universal rheological features; at nanotube concentration above a characteristic value $n_c \sim 2-3$ wt. % the effective elastic gel network is formed, while the low-concentration composite remains a viscous liquid. We use this rheological approach to determine the effects of aging and reaggregation.

DOI: 10.1103/PhysRevB.73.125422 PACS number(s): 81.07.−b, 81.05.Qk, 83.80.Hj

I. INTRODUCTION

The pursuit of well dispersed nanotubes into a given matrix is a fundamental problem that still hinders research and development a long time since they were brought to global attention.[1] Monitoring the quality of dispersion within a given system gives rise to additional problems. While clustering of spherical particles has been studied well, for both spherical and highly asymmetrical (platelets, rods, and fibers),[2–6] there are no reliable direct techniques of observing carbon nanotubes in the bulk of a composite suspension. All optical methods cut off below a length scale of $\sim 0.2-0.5$ μm; all electron microscopy methods (so prominent in observations of individual nanotubes) can only provide information about the sample surface, i.e., only representative for the selected fields of view. This leaves reciprocal space techniques and, more importantly, global indirect techniques of characterizing the dispersed nanocomposites. Each of these techniques suffers from the unavoidable difficulty in interpretation of results. A recent review gives a summary of such approaches, their strong and weak aspects, and prospects.[7]

If efficient and economically viable bulk processing of nanotube-polymer composites is to be realized, a well-developed understanding of responses to simple steady-state shear flow is required. In this paper we concentrate on the analysis and interpretation of rheological characteristics of nanocomposites at different stages of their dispersion and subsequent aging (tube reaggregation). Some rheological data has appeared in the recent literature[8–11] but to our understanding, no work has yet been undertaken to apply rheological data to characterize the state of dispersion directly, and moreover, to investigate the effect of conditions and mixing time on the quality of nanotube dispersion.

In itself, dispersion is a spatial property whereby the individual components (in this case nanotubes) are spread with the roughly uniform number density throughout the continuous supporting matrix. The first challenge is to separate the tubes from their initial aggregated assemblies, which is usually achieved by local shear forces. However, a homogeneous suspension ideally achieved after mixing is not necessarily a stable state: the removal of a shearing force may open the way to reaggregation. At very low concentrations, the conditions of an ideal-gas occur, when the dispersed objects do not interact with each other. However, for nanotubes with very high persistence length, the Onsager treatment of anisotropic suspensions[12] suggests that the crossover concentration when the rodlike objects start interacting and significantly biasing their orientational pair correlation can be very low indeed.[13,14] Experimental evidence suggests external hydrodynamic forces can also induce clustering in highly anisotropic suspensions.[15] There are several classical ways of surface treatment, which improves the colloidal stability of nanotubes;[7] in all cases it is more challenging than in usual sterically stabilized colloids because of the unusual depth of the primary van der Waals minimum due to the high polarizability of nanotubes. Many authors have suggested that when the loading of nanotubes is above a critical value, a network structure can form in the nanocomposite system during mixing.[8,10,16] Elastic gel, arising from such an entangled nanotube network,[17,18] may prevent individual tube motion and thus serve as an alternative mechanism of stabilization.

In this work we choose to work with untreated tubes, since our main goal is to examine the dispersion and reaggregation mechanisms. We believe that the state of dispersion in a given composite dispersion can be ascertained by measuring the global rheological properties of the system. The viscosity of the mixture has a direct correlation with the spatial and orientational distribution of nanotubes in the matrix. This can be used as a physical signal with which to monitor the quality of dispersion, as long as the interpretation of the rheological signal is calibrated. By studying the rheology of a viscous polymer mixed with nanotubes at different stages of dispersion and aging we aim to provide, for instance, an answer to the question of how long one should shearmix their nanotube-polymer sample to achieve a suitable level of dispersion. Our conclusions are somewhat surprising: the required mixing time is so long and the required mixing shear so high that one might question the quality of nanotube dispersion of many famous experiments in the last decade.

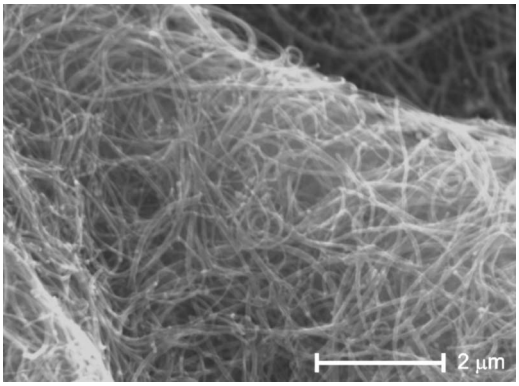

FIG. 1. A typical scanning electron microscopy (SEM) image of nanotube agglomerates from the supplier, showing the entangled nature of raw samples prepared by the CVD method.

The discussion of this work is split into three parts. First, after giving the details of sample preparation and measuring procedures, we give an overview on how the composite viscosities are affected by tube concentration and mixing time. Secondly, we develop a general interpretation of the frequency dependence of rheological data, and possible dispersion states have been correspondingly deduced, especially focusing on higher concentrations and elastic gel network formation. Finally, the stability of the dispersion state is discussed in the last part of this paper. In Conclusions, we cast a critical look at our own work as well as the claims of nanotube dispersion in the literature.

II. EXPERIMENTAL

Multiwalled carbon nanotubes (Nanostructured & Amorphous Materials, Inc.) are used with purity verified as >95%. These nanotubes, prepared by the method of catalytic vapor deposition (CVD), are found to be tangled in agglomerates, Fig. 1, in contrast to many other sources producing tubes in densely packed and aligned bundles obtained by the CVD technique. The manufacturer specified dimensions, tube length $L \sim 5-15$ μm and outer diameter $d \sim 60-100$ nm, are confirmed by direct SEM observation, also indicating the tube persistence length $l_p \sim 0.5-1$ μm. The pristine nanotubes were lightly ground by pestle and mortar prior to usage without surface-modification at any time during processing.

The physics of semiflexible "wormlike chains" (representing our tubes) in a solvent (our matrix) is well developed.[19] Given the parameters of diameter d, persistence length l_p, and total arc length L, we can estimate the characteristic overlap concentration, which theoretically marks the boundary between dilute (individual tubes in solution) and semidilute (overlapping tube coils) regimes. Explaining this in detail is not a task for us and we refer the interested reader to the polymer physics literature. The model result for the overlap volume fraction ϕ_c depends on whether one accounts for the so-called excluded volume interaction (i.e., prohibits tubes from crossing each other). It is often neglected in the first approximation, but we shall specifically need this excluded volume interaction to account for the elastic entangled network emerging in our system.[25] Therefore, the overlap volume fraction is estimated as $\phi_c \sim d^{7/5} l_p^{-3/5} L^{-4/5}$. For our tube parameters this gives the volume fraction $\phi_c \sim 0.003-0.008$. However, to make comparisons with our experiments (in which we measure the loading by the weight percent), we need to convert the volume fraction $\phi = V_{\text{tube}}/V_{\text{total}}$ into the weight fraction. Using the density of nanotubes, $\rho_{\text{tube}} \sim 2.1$ g/cm^3 (from the manufacturer data sheet), we estimate the overlap to occur at $n_c \sim 0.5-1.5$ wt. %. Above this concentration, the semidilute solution of self-avoiding chains becomes increasingly entangled and develops the elastic modulus.[19]

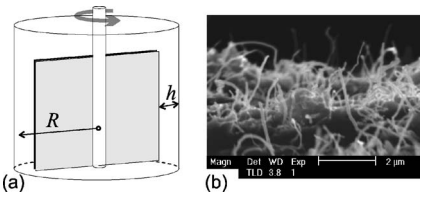

FIG. 2. (a) Scheme of the mixer container, with the relevant dimensions labelled for calculation of shear stress. (b) An SEM image of freeze-fractured surface of a well-dispersed 7 wt. % composite (t_{mix}=61 h).

The polymer matrix used throughout this work is PDMS (Polydimethylsiloxane) Sylgard 184$^{\text{TM}}$ from Dow Corning. We have not crosslinked the elastomer networks with the usual Sylgard curing agent, instead using only the PDMS compound as a well-characterized viscoelastic liquid. The compound has a molecular weight $M_w \sim 18.5$ kD, density $\rho \sim 1.2$ g/cm^3, and the apparent viscosity of 5.6 Pa s at 25 °C.

Batches of samples (each of about 2 g total weight) were prepared with different weight fractions: 0.5, 1, 2, 4, and 7 wt. %, by direct addition of the PDMS compound onto the dry nanotubes. The samples were dispersed by using an Ika Labortechnik mixer; the geometry of shear mixing is illustrated in Fig. 2(a), specifying the key dimensions used in the analysis below. Throughout the dispersion process, the rotation speed of the paddle was kept at 1000 rpm and the mixing temperatures kept at 30±0.5 °C. The high speed of mixing and comparably low mixing temperature should ensure that only stimulated dispersion and little spontaneous reaggregation to take place during mixing (see Ref. 20).

After a desired length of mixing time, aliquots of the sample were removed from the mixer and their rheological characteristics were measured immediately, as well as after different standing times (the period of time elapsed after the mixer has been switched off and before rheological tests were conducted). The standing samples were stored at room temperature.

According to the geometry of the mixer, the shear stress applied to the nanotube-PDMS mixture can be approximated as $\sigma \sim \eta R\omega/h$, where $R \approx 7$ mm and $h \approx 1.5$ mm are the radius and the gap indicated in the diagram, $\omega \approx 1.2 \times 10^5$ rad s^{-1} the angular frequency of the paddle and η is the viscosity of PDMS. The resulting estimate of shear stress is of the order of 1 MPa, increasing with the increasing nanotube loading. The ultimate tensile stress of single- and multiple-walled nanotubes is in the range of 200–900 MPa,[21–23] therefore, direct scission of the tubes is unlikely to occur during mixing.

Monitoring the quality of nanotube dispersion in a continuous polymer matrix is a perennial problem, with very few experimental techniques available to resolve it. Electron microscopy, which is the only method offering real-space resolution on the scale of nanotubes, is an inherently surface technique. Attempting to dissolve or ion etch the polymer to reveal the tubes, immediately leads to their reaggregation. Making samples very thin to allow transmission microscopy makes nanotubes interact with surfaces much more than with the bulk. Figure 2(b) shows the SEM image of a freeze-fractured interface of a well-mixed 7 wt. % polymer composite. It suggests the tubes are homogeneously dispersed, but is far from offering any proof of dispersion quality. The main point of our present work is to develop and alternative (rheological) quantitative method of monitoring the dispersion.

Rheological measurements were staged on a stress-controlled Rheometrics DSR (dynamic stress rheometer) connected to a water bath heater to ensure a consistent temperature of 30 ± 0.5 °C. A cone-and-plate geometry (25 mm diameter, 0.1 rad cone angle, gap 0.01 mm) was utilized and a stress-controlled (set at 100 Pa) frequency sweep was performed to monitor the linear viscoelastic response of each sample. In order to compare the characteristic viscosity of each composite, we chose the frequency of 50 Hz.

For this cone-plate shear geometry we define the Reynolds number by $\mathrm{Re}\approx\dot{\gamma}z^2\rho/\eta$, with ρ the PDMS mass density, $\dot{\gamma}$ the strain rate, and z the average distance between the test plates. We find $\mathrm{Re}\leqslant10^{-3}$ for all strain rates used throughout our experiments.

We ensured (by comparing the data at different shear rates) that the rheometer provides oscillatory shear measurements of linear response, with the real and imaginary viscosities [$\eta'(\omega)$ and $\eta''(\omega)$, respectively]. The equivalent information contained in the storage and loss shear moduli [$G'(\omega)$ and $G''(\omega)$] is useful for identifying gel properties and jamming of clusters.

III. RESULTS AND DISCUSSION

A. Mixing time of dispersion

In order to determine the effect of mixing time on the degree of nanotube dispersion, three identical experiments were performed for samples with 1 wt. % concentration of nanotubes, with the results shown in Fig. 3. Each test was conducted on an aliquot of the composite after a certain time of continuous mixing of a sample; this was repeated for three separate mixtures. The rheological test protocol involves taking each sample through a full frequency sweep and measuring its shear response; the plot only shows the value of η' sampled at one frequency. The values of the viscosity obtained for the short mixing times ($t<100$ min) have erratic values, such that no trend can be assigned to the viscosity variation with increasing mixing time. We shall discuss the origins of this effect at greater detail below. Presently, it is important to note that after a certain time of mixing, these erratic values turn to a consistent value of composite viscosity, which is the same in different experiments and not much affected by further mixing. We interpret this characteristic

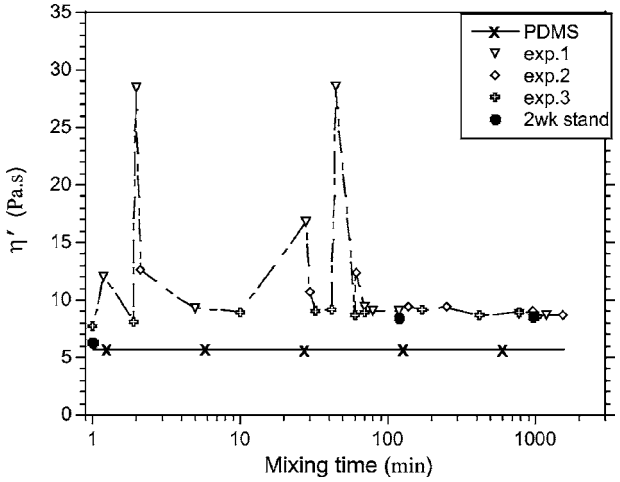

FIG. 3. Plot of the real viscosity η', sampled at fixed frequency 50 Hz, against the time of mixing for the 1 wt. % nanotube-PDMS sample. Three different experiments have been carried out and the results shown on the same plot. The data shows that for $t_{\mathrm{mix}}<\sim100$ min, the viscosity reading is erratic; mixing for longer periods leads to reproducible well-dispersed composite. Black dots show the selected samples tested after 2 weeks standing.

time, t^*, as the minimal time required to achieve the complete dispersion at the given concentration of tubes and the mixing shear stress.

The comparison of different experiments for a 1 wt. % sample in Fig. 3 is a good illustration of universality. Overall, such change in viscosity with mixing time occurs for all mixtures investigated, Fig. 4. Note that the axes scale in Fig. 3 is linear-log (to capture the whole time range and emphasize the variations in η'), while the log-linear axes are used in Fig. 4 (to focus on the early times and allow all viscosity data on the same plot). In Fig. 4, for each sample, the data

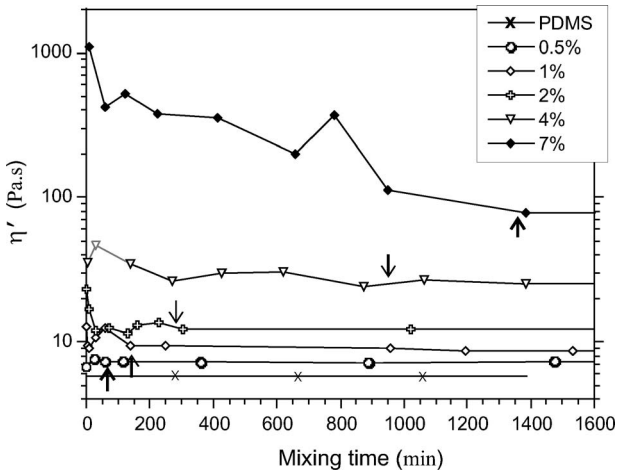

FIG. 4. Plot of the real viscosity, η' at 50 Hz, against the time of mixing, for a range of different weight fractions of nanotubes in the composite. The viscosity axis is logarithmic to allow all samples to fit on the same plot, since the viscosity increase with tube concentration is significant, while the time axis is linear to allow low concentrations to be resolved. The arrows mark the critical time t^* for each concentration.

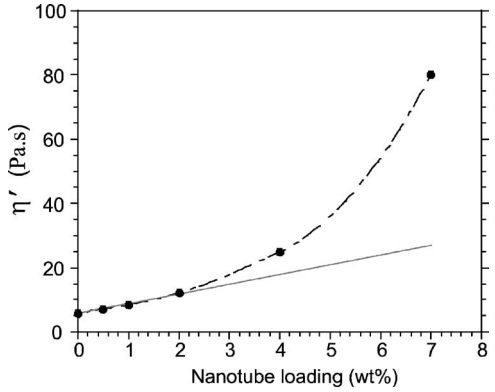

FIG. 5. Plot of the dispersion plateau viscosity (at 50 Hz) against the weight fraction of nanotubes in the composite. The solid line shows the initial linear (non-interacting) regime; the dashed line is a guide to an eye in the nonlinear (entangled) regime.

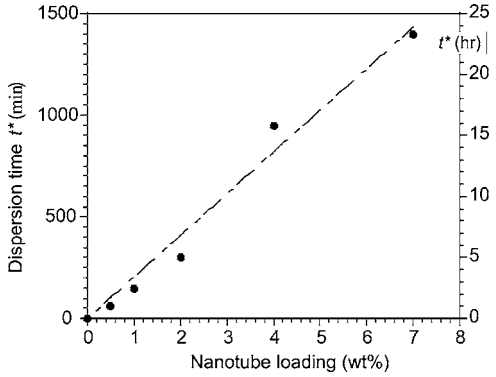

FIG. 6. Plot of the critical time for dispersion t^* obtained from data in Fig. 4, against the weight fraction of nanotubes. The right axis shows the same time in hours. The dashed line is the linear fit $t^* \propto n$ (see text).

points at very long times are not shown (e.g., $t_{\text{mix}}=61$ h for 7 wt. %) since no further change in η' was observed.

The key features of the dispersion process, the large increase in overall viscosity with nanotube loading, the erratic values at short mixing times and the consistent reproducible viscosity reading for each composite, dispersed for $t>t^*$, are reproduced for each sample. Although we do not show the corresponding plots, it was found that this characteristic time for the onset of the stable region (i.e., the signature of the complete dispersion) was independent of the sampling frequency and is equally evident true for both η' and η''.

In general, erratic behavior for short-time-mixed (i.e., incompletely dispersed) composites implies the nanotube clusters have a large variation in sizes and concentration across the bulk mixture. Each batch of sample can have its own dispersion characteristic after being mixed for a short time. This results in an unavoidably unpredictable results of our rheological measurements.

Clearly, every batch of the same concentration should tend to the same dispersion state after being mixed long enough, $t>t^*$. The resulting dispersion should consist of a fairly uniform distribution of nanotube, which does not change with further mixing and yields a specific and reproducible rheological response as indicated by the plateau regimes in Fig. 4. Two important results can be further extracted from this data: the dependence of the final plateau viscosity, and of the critical mixing time t^*, on the tube concentration. These are presented in Figs. 5 and 6. The concentration dependence of the final plateau value of the dispersion viscosity η_s' shows the expected linear increase at low concentrations, corresponding to the noninteracting Einstein-like suspension viscosity; the line in Fig. 5 is $\eta'=\eta'_{\text{PDMS}}(1+103.5\phi)$, where ϕ is the volume fraction of nanotubes calculated from the value of wt. % in the plots.[26] At concentrations above $n^*\sim 2$ wt. % the deviations from the linear regime become noticeable indicating the tube interactions and eventually entanglements in the dispersed composite.

Figure 6 shows a fairly linear correlation between the critical mixing time t^* and tube concentration. The following simple argument suggests that this is an expected feature: Let us define $dE(n,t)$ be the elementary energy needed to disperse one nanotube in a composite with a given environment characterized by the nanotube loading n and mixing time t. Similarly, let $P(n,t)$ be the power transmitted during the shear mixing, where t is the time of mixing ($t<t^*$). Thus

$$\int_0^n dE(n,t) = \int_0^t P(n,t)dt.$$

To simplify this crude analysis, we define $\bar{E}(n)$ as the average constant energy needed to disperse a nanotube, and similarly $\bar{P}(n)$ as the average power. This will lead to $n\bar{E}(n)=\bar{P}(n)t^*$ and, therefore, $t^*=n[\bar{E}(n)/\bar{P}(n)]$. Since physically, both $dE(n)$ and $P(n)$ describe the same process, it is not surprising that their ratio is nearly constant and the primary n dependence is linear, as indeed is seen in Fig. 6.

B. Dispersion rheology

1. Clusters at $t_{\text{mix}}<t^*$

It has already been stated in the previous section that the rheological response for $t_{\text{mix}}<t^*$ is erratic. This requires some detailed discussion. Occasionally, in such poorly dispersed samples, η' is obtained several orders of magnitude greater than what would otherwise be expected (see Fig. 3). In Fig. 7 we show two such measurements, as a frequency sweep, for a 2 wt. % (mixed for 2 min) and a 4 wt. % (mixed for 1 h) samples each. In each sample, one of the measurements is a meaningful representation of a complex-fluid response. The other (very high) reading is identical for different samples and reflects an arrest of the rheometer plates when a nanotube cluster is wedged between them. Such poorly mixed composites are invariably found to contain visible nanotube clusters, which are the main reason for the accidentally high viscosity reading. When such clusters are so large as to block the rheometer plates (minimal cone-and-plate gap is 0.01 mm), the measurement is obviously flawed. The scanning electron microscope (SEM) image of one typical cluster in Fig. 8 shows a size of 0.05 mm and a much more compacted structure in comparison with the initial entangled tube agglomerates (Fig 1). When such plate

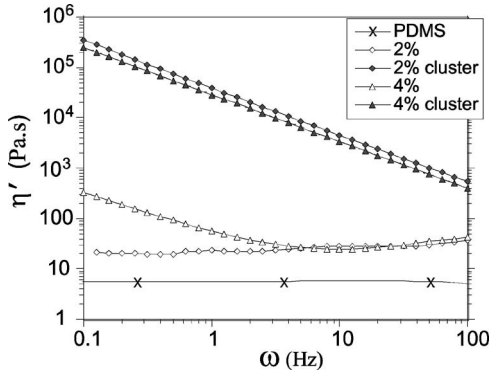

FIG. 7. Frequency sweep of viscosity for 2 and 4 wt. % samples mixed for $t_{mix} < t^*$. The bold symbols show the results when the sample aliquot in the rheometer was found to contain visible nanotube clusters: note the extremely high values of (arrested) η', the same for different samples.

blocking occurs, the viscosity readings are obviously unaffected by the nanotube concentration. Longer mixing-times ensures the clusters are broken down into a homogeneous dispersion, hence no further erratic behavior is observed.

2. Well dispersed state $t_{mix} > t^*$

The well dispersed states can be characterized by their reproducible profile of the rheological linear response. Figures 9 and 10 give a summary of these results, in both η' and G' representations. Increasing nanotube concentration increases the values of η', and also causes it to become more frequency dependent. The 0.5, 1, and 2 wt. % samples, just like the pristine PDMS, exhibit a nearly frequency-independent Newtonian plateau in the range of frequencies studied. These systems are dilute enough so that the effect of hydrodynamic interaction between tubes is negligible. There

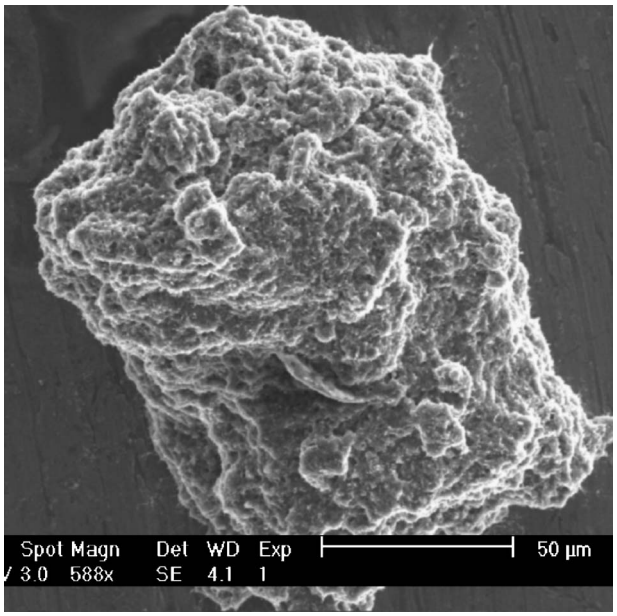

FIG. 8. SEM image of a typical compact nanotube cluster found in a sample mixed only for a few minutes.

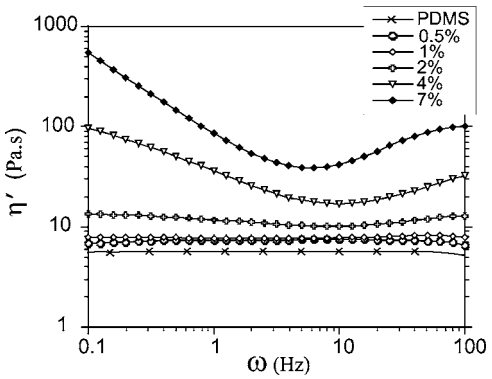

FIG. 9. Summary for the dynamic viscosity $\eta'(\omega)$ against frequency for well-dispersed samples of different concentrations.

is a significant change in the viscosity profiles between 2 and 4 wt. %, which suggests a major change in nanocomposite structure. Note that these are the concentrations at which we have verified the onset of nanotube interactions, see Fig. 5.

In order to identify the subsequent change in microstructure, we plot the storage shear modulus G' against frequency, Fig. 10. This is discussed in more detail in the next section. Here we only wish to attract the attention to the emerging rubber plateau, the static gel modulus $G'(\omega \to 0)$ for highly interacting nanotube dispersions.

Both our G' and η' values (in the well-mixed state) are $\sim$1 to 2 orders of magnitude lower for the same concentration of nanotubes than the results in the literature.[8,14] This is almost certainly due to the fact that our PDMS matrix has lower initial viscosity than the other systems investigated. However, in view of our findings about the erratically high values of response moduli in the state with insufficient tube dispersion (at $t < t^*$), one has to be cautious about the details of preparation of polymer nanocomposites: have the specific polymer-nanotube sample been mixed for a sufficient time at a given shear stress of mixing? Such a question is rarely addressed in the current literature, making comparison difficult.

The change in rheological behavior as concentration of tubes increases, similar to those presented in Figs. 9 and 10 have been reported for other nanotube (single- or multiple-

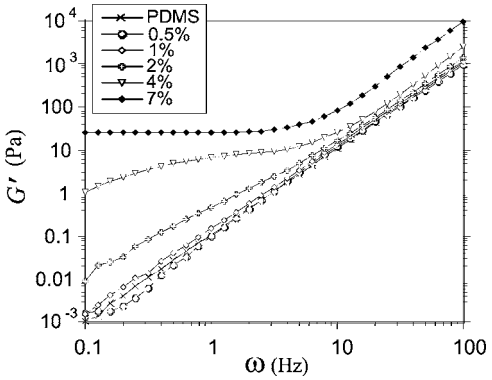

FIG. 10. Summary for the storage modulus $G'(\omega)$ against frequency for well-dispersed samples of different concentrations. Note the emerging low-frequency rubber plateau in G' at high tube concentrations.

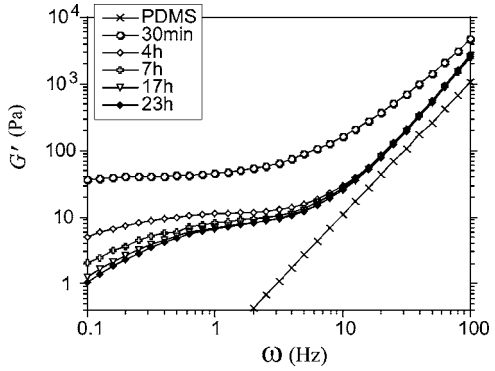

FIG. 11. Data of G' against frequency for 4 wt. % samples mixed for different times (tested immediately after mixing). Non-representative profiles (similar to "cluster" curves in Fig. 7) due to erratic behavior at $t<t^*=16$ h have been removed for clarity.

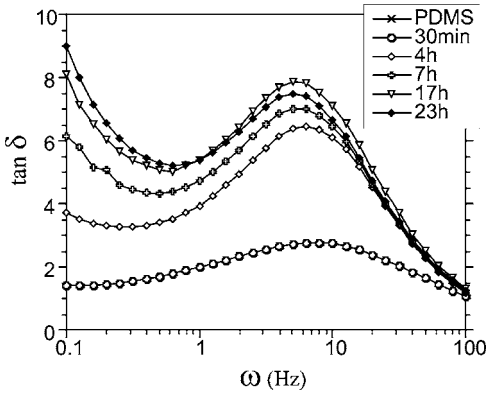

FIG. 12. Data for tan δ against frequency for 4 wt. % samples mixed for different times (tested immediately after mixing). Non-representative profiles due to erratic behavior at $t<t^*=16$ h have been removed for clarity.

walled) polymer composites and is often called the "percolation threshold."[8] More precisely, one might call the emergence of the static gel network the mechanical percolation threshold, so as to differentiate it from the more traditional electrical percolation.[10] Again, there are large discrepancies reported in the literature for such mechanical percolation concentrations, even for the same system. A reason for this might well arise because of two distinct possibilities. First, by forming a well dispersed and homogenous ($t_{\mathrm{mix}}>t^*$) *network* of nanotubes one may reach, and exceed, the entanglement limit. In this case the rheological response would become that of an elastic solid. Secondly, mechanical percolation could take place when individual aggregates, or tube clusters (at $t_{\mathrm{mix}}<t^*$), come in contact and form force chains. This second type of aggregate-mediated jamming may well be responsible for much higher threshold concentrations and moduli previously reported. Better dispersed samples of very long nanotubes will naturally provide much lower percolation thresholds.

3. Mixing at high tube concentrations

As the weight fraction of nanotubes increases, the mixing mechanism and the resulting dispersed structure also becomes more complicated. For instance, for 7 wt. % samples, empirical observations suggest that the mixture was not continuous during mixing: for the first few hours of mixing, clusters were sticking to the walls of the container. Some clusters were then observed to migrate to form larger structures (the whole process resembled the mixing of a slurry). As the mixing time lengthened ($t_{\mathrm{mix}}>10$ h), large clusters "connected" back with the main mixture and were eventually broken down.

The most significant change associated with the critical concentration of nanotubes above which tube interactions are relevant is the presence of an entangled elastic network structure as the state of full dispersion is approached, $t\sim t^*$. Evidence for this is shown by the rubber plateau in the storage modulus at $\omega\rightarrow 0$ and also in the peaks in the loss factor tan δ. Because the relatively high stiffness (large persistence length) of nanotubes, the amount of entanglements that can form are a lot less compared to that of common polymers (thus relatively low G' of the network). On the other hand, the high polarizability of the tubes also implies that once these entanglements are formed, they are hard to disconnect. All the tubes are connected by these physical crosslinks and form a homogeneous network structure in the PDMS matrix. The rise in the tan(δ) peak with increasing mixing time is a useful empirical method by which to confirm and quantify nanotube dispersion.

In general, the change of $G'(\omega)$ profile for the 4 wt. % composite, Figs. 11 and 12, is similar to that of the 7 wt. % sample. However, the latter has a more pronounced change in its rheological response as the mixture homogenizes. Figure 13 shows a distinct difference in $G'(\omega)$ between the viscous PDMS liquid and the essentially solid nanotube composite after just 10 min of mixing. We associate the high plateau ($G'\sim 100$ kPa) with a state of colloidal glass, or a rheologically jammed state of tube clusters. As the time of mixing increases, we observe the characteristic step of a glass transition travel through the $G'(\omega)$ plots from the low to the high frequencies. The end, in the well-mixed dispersion, is a much lower rubber plateau ($G'\sim 20-40$ Pa) of the homogeneous entangled nanotube network. The corresponding movement of the tan δ peak in Fig. 14 tells essentially the same story.

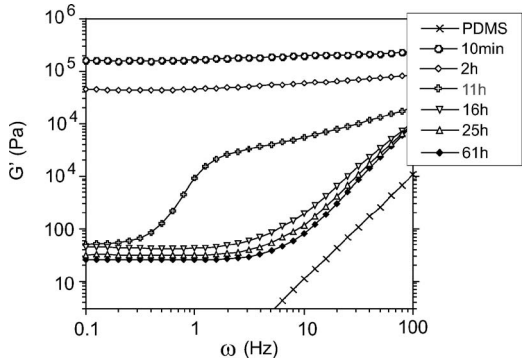

FIG. 13. Data for G' against frequency for 7 wt. % samples mixed for different times (tested immediately after mixing). Non-representative profiles due to erratic behavior at $t<t^*=23$ h have been removed for clarity.

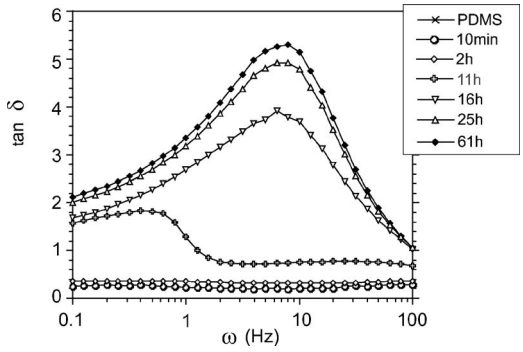

FIG. 14. Data for tan δ against frequency for 7 wt. % samples mixed for different times (tested immediately after mixing). Nonrepresentative profiles due to erratic behavior at $t<t^*=23$ h have been removed for clarity.

C. Reaggregation and aging

1 and 7 wt. % samples were selected to test the stability of homogeneous dispersion, samples with nanotube concentration below and above the critical entanglement value. The results for the two-week aging of 1 wt. % composite are in fact shown in Fig. 3, back in Sec. III A. The sample mixed for just 2min ($t_{\mathrm{mix}} \ll t^*$) we have seen in a large drop in η' upon standing for 2 weeks, essentially recovering a pure PDMS value. In contrast, very little change in viscosity was registered for the same aging of well-mixed samples, at $t_{\mathrm{mix}} > t^*$. The apparent conclusion is that sparse noninteracting nanotubes dispersed in a viscous matrix do not have enough Brownian mobility to reaggregate.

Above the percolation concentration, the 7 wt. % composite exhibits a very different aging behavior. Figure 15 shows two groups of measurements, for the samples mixed for a short time ($t_{\mathrm{mix}}=1$ h, labeled T1 in the plot), for the intermediate stage of mixing ($t_{\mathrm{mix}}=16$ h, labeled T2), and for the well-dispersed composites ($t_{\mathrm{mix}}=61$ h, labeled T3). The T1 response function $G'(\omega)$ shows only weak aging and remains similar to the high value of colloidal glass modulus, see the top curves in Fig. 13. This observation is consistent

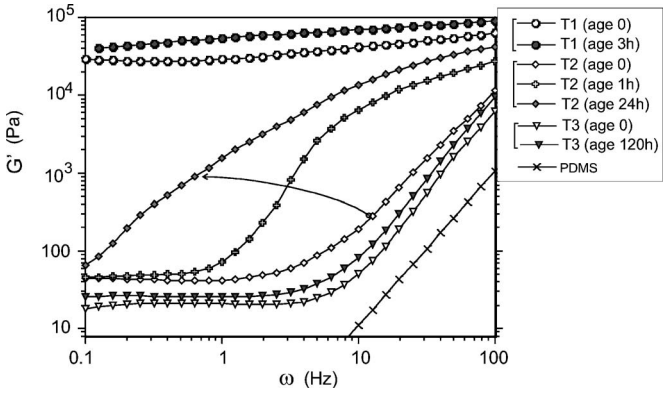

FIG. 15. Plots of G' against angular frequency for 7 wt. % samples. Three groups of data are labeled: T1 for the short mixing time $t \ll t^*$, T2 for the intermediate state of mixing ($t \leqslant t^*$), and T3 for the well-dispersed composite ($t \geqslant t^*$). The age of each sample is labeled in the legend.

with the idea of a dynamical glassy state of jammed nanotube clusters.

The T2 response function $G'(\omega)$ evolves most significantly with the aging time. This is highlighted by the arrow drawn on the plot in Fig. 15. The freshly made sample has the response of an entangled elastic gel, with the plateau modulus at $\omega \to 0$, as discussed above. Although this was not yet a well-dispersed sample, the main features of tube entanglement have already became apparent (see the G' curve second from the bottom in Fig. 13). However, as this sample ages, the rheological transition in this metastable gel moves to the lower frequencies. In effect, we are observing the movement of the dynamic glass transition across the plot in Fig. 15. It seems reasonable to assume that after a very long time the modulus would revert to the colloid glass values characteristic of the jammed cluster system T1.

Finally, the rheological signature of a well-dispersed sample T3 shows, once again, only a very small aging in spite of a very long time allowed for this sample to stand (6 days). The rubber plateau modulus $G'(\omega \to 0) \sim 20$ Pa remains almost unchanged, as does the frequency of the transition. We may conclude that the entangled network of nanotubes, with no clusters left to act as seeds for reaggregation, represents a very deep energy well of a dispersion metastable state.

In order to explain the phenomena observed in the standing samples with low concentrations, both sedimentation and reaggregation processes should be considered. For spherical particles, the ratio of gravitational to Brownian forces $a^4 \Delta\rho g/(k_B T)$ should be less than unity so as to avoid sedimentation. Applying this idea to our system, with the density difference between compacted nanotubes and the PDMS of order $\Delta\rho \sim 0.6$ g/cm^3, it shows that any clusters of sizes greater than ~ 1.5 μm would tend to settle at room temperatures. The high viscosity of the medium may require a long time for the effect to become noticeable, especially for smaller sized clusters.

By comparing Figs. 15 and 13, it is clear that the relaxation, or aging, is a reverse process of dispersion, the sample T2 clearly being dispersed into a metastable state prone to relaxation. Further development of an entangled elastic network would serve to stabilize the homogeneous dispersed state, so that no substantial relaxation is observed within the duration of our experiment—but it is nevertheless going to happen in the same way.

The implication of the dispersion aging is important to note. First, even an ideal homogeneous dispersion achieved when $t_{\mathrm{mix}} \geqslant t^*$ may well disappear after a time, unless further processing steps are taken to "freeze-in" the dispersed structure, e.g., by chemical cross linking of the polymer matrix. Storage conditions should be changed so as to minimize the alteration, e.g., by cooling the matrix below the polymer glass transition. Secondly, in order to use rheological data to study the effect of mixing time on dispersion, special caution should be taken for the higher loaded samples (>2 wt. % in our case) due to the relaxation processes that are sensitive to standing times.

IV. CONCLUSION

Experiments have shown that a critical time t^* is needed to disperse carbon nanotubes in a polymer melt, reaching a

consistent and reproducible state of such a dispersion. Below this characteristic time, the composite system is full of dense tube clusters (often smaller than an optical microscope resolution). This manifests itself in erratic rheological properties, depending on accidental jamming of the resulting "colloidal glass" system. Dispersions mixed for a time longer than t^* appear homogeneously mixed, with their rheological behavior shows no evidence of jamming. We may only hope a complete dispersion has been achieved at mixing times above t^*. One cannot exclude a presence of consistently small tube clusters or bundles, and there is no unambiguous technique to confirm or disprove this. However, a homogeneous dispersion is suggested by images of freeze-fractured surfaces, Fig. 2(b), and by comparing the estimates of semiflexible overlap and entanglement concentrations with our rheological measurements. For all practical purposes we regard our composite at $t > t^*$ as completely dispersed, which is hardly the case in the present literature.

The critical time of mixing, t^*, is a function of nanotube concentration and the shear stress in the mixing device (itself a function of vessel geometry and the viscosity of the polymer matrix). Although we have not done such a study, it is quite obvious that the shear stress energy delivered to the particles during mixing ($\sim 10^6$ J/m^3 in our case) has to exceed the van der Waals force of their attraction in the contact region (crudely estimated as, $\sim 10^4$ J/m^3, from Ref. 24). Below this shear energy density one cannot hope to achieve dispersion no matter how long the mixing is.

The second important parameter in nanotube dispersion is their concentration. Well-dispersed systems possess very different rheological properties below and above the concentration of "mechanical percolation" (we use this term reluctantly, only because it seems to be in heavy use in the literature: the true percolation is a somewhat different physical process). At low concentrations, noninteracting nanotubes homogeneously dispersed in the polymer matrix appear quite stable against reaggregation (provided the matrix viscosity is high enough to suppress fast Brownian motion). The rheology of such dispersions remains that of a viscous liquid, with the observed steady-state viscosity a linear function of tube concentration (the slope of this dependence, much higher than the classical Einstein's 2.5, is certainly due to the profound shape anisotropy of nanotubes).

At concentrations above the threshold of order 2–3 wt. % in our case we see a clear emergence of an elastic gel of entangled nanotubes in their homogeneously dispersed state. This agrees favorably with an estimate of overlap concentration $n_c \sim 1.5$ wt. % made in Sec. II (considering the inevitably crude nature of n_c estimate). The rheological characteristics of these composites have a distinct rubber modulus G' in the limit of zero frequency. We also note a characteristic superposition between the mixing time and the frequency of rheological testing, similar to the time/temperature superposition in classical glass-forming polymers. Here we find the transition between the colloidal glass state of jammed tube clusters at short mixing times, and the weakly elastic state of an entangled nanotube gel. We hope these results, as well as the brief study of reaggregation and sedimentation of dispersed polymer nanocomposites, will contribute to a more rigorous and quantitative approach of preparation and analysis of carbon nanotube dispersions.

ACKNOWLEDGMENTS

We thank S. F. Edwards, A. Craig, and A. R. Tajbakhsh for insightful discussions. This work was carried out with the support of the EPSRC, the ESA-ESTEC (18351/04) and a CASE award from Makevale, Ltd.

[1] S. Iijima, Nature (London) **354**, 56 (1991).
[2] J. Persello, A. Magnin, J. Chang, J. M. Piau, and B. Cabane, J. Rheol. **38**, 1845 (1994).
[3] E. K. Hobbie, Phys. Rev. Lett. **81**, 3996 (1998).
[4] D. Fry, T. Sintes, A. Chakrabarti, and C. M. Sorensen, Phys. Rev. Lett. **89**, 148301 (2002).
[5] S. Lin-Gibson, G. Schmidt, H. Kim, C. C. Han, and E. K. Hobbie, J. Chem. Phys. **119**, 8080 (2003).
[6] A. Mohraz, D. B. Moler, R. M. Ziff, and M. J. Solomon, Phys. Rev. Lett. **92**, 155503 (2004).
[7] S. V. Ahir and E. M. Terentjev, in *Polymeric Nanostructures and Their Applications*, edited by H. S. Nalwa (American Scientific Publishers, New York, 2005).
[8] P. Potschke, T. D. Fornes, and D. R. Paul, Polymer **43**, 3247 (2002).
[9] S. Lin-Gibson, J. A. Pathak, E. A. Grulke, H. Wang, and E. K. Hobbie, Phys. Rev. Lett. **92**, 048302 (2004).
[10] F. M. Du, R. C. Scogna, W. Zhou, S. Brand, J. E. Fischer, and K. I. Winey, Macromolecules **37**, 9048 (2004).
[11] P. Potschke, A. R. Bhattacharyya, and A. Janke, Eur. Polym. J. **40**, 137 (2004).
[12] P. G. de Gennes and J. Prost, *Physics of Liquid Crystals* (Oxford University Press, Oxford, 1994).
[13] M. F. Islam, A. M. Alsayed, Z. Dogic, J. Zhang, T. C. Lubensky, and A. G. Yodh, Phys. Rev. Lett. **92**, 088303 (2004).
[14] W. H. Song and A. H. Windle, Macromolecules **38**, 6181 (2005).
[15] C. F. Schmid and D. J. Klingenberg, Phys. Rev. Lett. **84**, 290 (2000).
[16] M. S. P. Shaffer, X. Fan, and A. H. Windle, Carbon **36**, 1603 (1998).
[17] I. A. Kinloch, S. A. Roberts, and A. H. Windle, Polymer, **43**, 7483 (2002).
[18] S. B. Kharchenko, J. F. Douglas, J. Obrzut, E. A. Grulke, and K. B. Migler, Nat. Mater. **3**, 564 (2004).
[19] R. H. Colby and M. Rubinstein, *Polymer Physics* (Oxford University Press, Oxford, 2003).
[20] C. A. Martin, J. K. W. Sandler, M. S. P. Shaffer, M.-K. Schwarz, W. Bauhofer, K. Schulte, and A. H. Windle, Compos. Sci. Technol. **64**, 2309 (2004).
[21] L. S. Schadler, S. C. Giannaris, and P. M. Ajayan, Appl. Phys. Lett. **73**, 3842 (1998).
[22] J. P. Salvetat, A. D. Briggs, J. M. Bonard, R. R. Bacsa, A. J.

Kulik, T. Stöckli, N. A. Burnham, and L. Forró, Phys. Rev. Lett. **82**, 944 (1999).

[23] D. A. Walters, L. M. Ericson, M. J. Casavant, J. Liu, D. T. Colbert, K. A. Smith, and R. E. Smalley, Appl. Phys. Lett. **74**, 3803 (1999).

[24] M. J. Bronikowski, P. A. Willis, D. T. Colbert, K. A. Smith, and R. E. Smalley, J. Vac. Sci. Technol. A **19**, 1800 (2001).

[25] Potential energy of excluded volume interactions, $U \sim kTn^2d^3R^3 \approx kTdL^2/R^3$ is balanced against the entropic free energy $F \sim kTR^2/(l_pL)$ of the semiflexible chain, giving the chain size $R_g \sim (l_pd)^{1/5}L^{3/5}$. The overlap is then at a volume fraction $\phi_c \sim d^2L/R_g^3$.

[26] There is no point comparing the slope of $(1+103.5\,n)$ with, e.g., a classical result for the dispersion of rigid rods: our tubes are anything but rods, cf see Fig. 1, and the more appropriate models of dilute semiflexible polymer solutions are too ambiguous to offer a reliable number.